An Analysis on the Ability of Colloidal Silver to Act as a Biosensor for the Steroid Testosterone via Host-Guest Interactions

Daniel J. Buker
Senior Comprehensive Project
Allegheny College, Class of 2017



Allegheny College
Department of Biochemistry

An Analysis on the Ability of Colloidal Silver to Act as a Biosensor for the Steroid Testosterone via Host-Guest Interactions

Daniel J. Buker
Senior Comprehensive Project
Allegheny College, Class of 2017

A Senior Comprehensive Project in Partial Fulfillment of the Requirements for a Bachelor of Science Degree from Allegheny College

Committee Members:
Dr. Alice Deckert (Advisor)
Dr. Tricia Humphreys
Dr. Timothy Chapp

I hereby recognize and pledge to fulfill my responsibilities as defined in the Honor Code and to maintain the integrity of both myself and the College community as a whole.

_____

Pledge

TABLE OF CONTENTS

ACKNOWLEDGEMENTS **1**

ABSTRACT **2**

INTRODUCTION **3**

TESTOSTERONE 3
SILVER COLLOID NANOPARTICLES 6
AGGREGATION AND DISAGGREGATION 9
HOST-GUEST CHEMISTRY 9
SYNTHESIS OF BCD CAPPED NANOPARTICLES 11
CENTRIFUGATION 12

EXPERIMENTAL METHODS **14**

MATERIALS AND HAZARDS 14
NANOPARTICLE PREP 14
CENTRIFUGATION TECHNIQUE 15
TESTOSTERONE ASSAYS 16

RESULTS **16**

TESTOSTERONE OVERLAYS 17
NORMALIZED EXTINCTION TREND 18
PEAK WIDTH TREND 21
ETHANOL STANDARDS 21
RS-S OVERLAY 22

DISCUSSION **22**

CONCLUSION **28**

REFERENCES **29**

Acknowledgements:

Mom and Dad, words cannot adequately describe how much you mean to me. Since day one, you have pushed me to become a better person and truly reach my potential. Without your constant support and love, I doubt I would have made it this far. Thank you so much for everything you have done for me and continue to do for me. I love you both.

Mindy, thank you for being the best big sister a guy could ask for. Even though we've had plenty of sibling-style fights, you have always been there for me and supported me in every way possible. Congratulations on your engagement, I love you.

Dr. Deckert, thank you so much for everything you have done for me over the past 4 years. From FS101 to my senior comp, you have always driven me to improve upon myself as not only a scientist, but as an individual as well. Thank you for allowing me to design and complete a project on my own, while also providing support and wisdom when needed. I am sure I will use the knowledge and skills you have given me throughout my career as a biochemist. Thank you.

Dr. Nelson, I wanted to take this time to thank you for all of the opportunities you have given me in the past year and a half. Thank you so much for allowing me to research with you over the summer and continue working with you as a teaching assistant. The skills I learned in your lab have made me into a well-rounded scientist with knowledge of both chemistry and biology related lab work. Thank you for allowing me to grow as a scientist.

Dr. Chapp, Dr. Humphreys, thank you for taking the time to read my senior thesis as well as listen to my presentations. The feedback I have received from both of you have made me think of my thesis in different ways and improve upon my laboratory skills. Thank you for being my senior thesis committee.

Roomates and Friends, thank you for all of your support and advice during my college career. We have had some great times together and I hope we will continue to do so after graduation.

Abstract:

This research project focused on using host-guest chemistry between β-Cyclodextrin and testosterone to aggregate silver nanoparticles and observe changes in their Localized Surface Plasmon Resonance (LSPR) band absorbance and wavelength. The concentrations tested mimicked that of physiological testosterone with the hopes of creating a calibration curve to accurately measure testosterone levels as a function of the optical changes of the nanoparticles. The nanoparticles were prepared with β-Cyclodextrin attached to act as a linker between particles when testosterone was introduced to the system. An array of testosterone and Reichstein's substance S, a testosterone derivative, samples were prepared and added to the colloidal solutions. The preliminary findings showed changes in the absorbance of a secondary shoulder peak of the UV-Visible spectrum for each sample when normalized to a set wavelength point. There was also an increase in the peak width of the secondary peak after the spectrum was mathematically simulated into two Gaussian distributions. Both of these changes were observed after testosterone was added, but not Reichstein's substance S. This biosensor appears to detect testosterone without also detecting derivatives with more polar substituents. According to these preliminary results, silver nanoparticles paired with host-guest reactions show promise in acting as a biosensor for the steroid testosterone.

Introduction:

Hormones and steroids are important signal molecules that are involved in several aspects of the biochemistry of the human body. One specific steroid, testosterone, is incredibly important for human functionality and needs to be consistently monitored to ensure the health of a person. Testosterone (T) is an anabolic steroid that occurs naturally in both males and females. This molecule is classified as an anabolic steroid due to its functionality as a signal molecule for producing larger, more complex molecules. Testosterone's anabolic effects are most closely associated with the development of skeletal muscle.[1] Although this steroid is present in both sexes, it is most important in the development of muscle mass and secondary sex characteristics in young males. Both high and low levels of T can be a cause or indicator for health issues. High levels of testosterone can be an indicator of low levels of HDL or "good" cholesterol in the body due to the fact that T is synthesized from cholesterol. Low levels of HDL are a precursor for heart issues and strokes. HDL transports LDL or "bad" cholesterol to the liver for reprocessing and also helps maintain the condition of the inner walls of blood vessels.[2] Low levels of T impair sex drive and reproductive function as well as muscle development. T can appear in the body either as a free molecule or bound to transport proteins. The two most common transport proteins for T are albumin and Sex Hormone Binding Globulin (SHBG). These proteins inhibit the activity of T until the hormone is delivered to a specific location.[3]

Testosterone is also known as an androgenic hormone, meaning this molecule follows the androgenic hormone signaling pathway. Androgen molecules are important for sexual development and additional muscle development.[4] In this case, T is acting as a signal molecule and is crucial in the sexual development of males at the transcriptional level. The hormone is transported to certain cells by the transport proteins discussed above. T is then released by the

proteins and can diffuse through the cell membrane where it later binds to an androgen receptor (AR) protein. The binding of T to the receptor protein activates heat shock proteins or HSPs, which facilitate the transport of the T-AR complex into the nucleus of the cell. This complex then proceeds to bind to the transcription machinery including RNA polymerase and acts as a transcription factor for genes associated with sexual development or spermatogenesis.[5] A graphical representation of this process appears in figure 1.

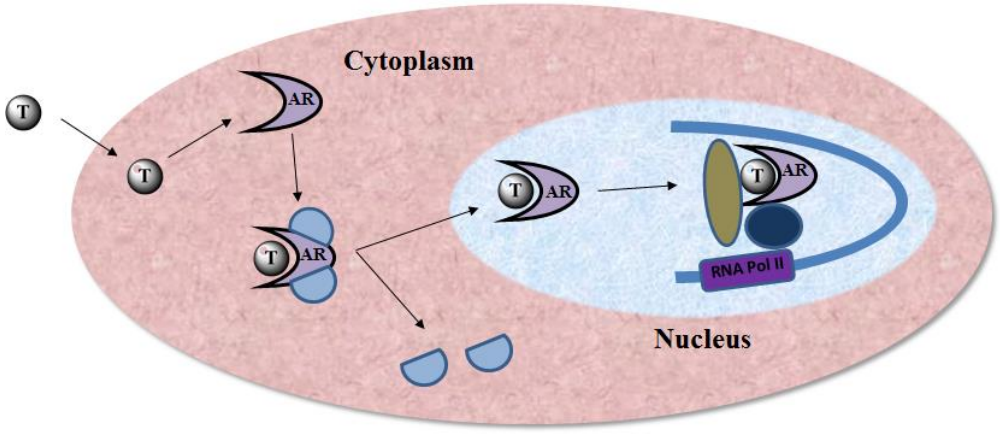

Figure 1: Cartoon displaying the basic concepts behind the androgenic hormone receptor pathway. The T molecules represent testosterone, the crescents labeled AR represent the androgen receptor proteins, and the blue semi-circles depict HSPs. Un-labeled ovals represent the additional transcription factors required for transcription located on a cartoonish depiction of DNA.

One study performed by *Nazareth and Weigel* delved deeper into this signal pathway to discover that transport of the androgen – androgen receptor complex is heavily dependent on the phosphorylation of the androgen receptor.[6] Phosphorylation of the receptor occurs after the androgen or T is bound. The study discovered that phosphorylation of the androgen receptor can occur independently of T-binding due to either an excess of certain kinases or absence of phosphatases. This occurrence is very commonly associated with over developed prostates and

in turn, prostate cancer. This study further highlights the importance of detecting testosterone levels and ensuring the androgen receptor pathway is functioning properly.

There is already an effective test for T in the blood stream known as the serum testosterone test which tests for the total amount of T in the body. This includes free T and T bound to proteins. Although this method is universally accepted as an effective way to measure T levels, I believe it may be just as important to test for the levels of free T separate from bound T. Prior literature states several methods of detecting biologically active T, however, there are discrepancies between certain methods depending on circumstances such as pregnancy and SHBG concentration.[7] Other, more accurate, techniques are time consuming and may not be suited for clinical testing.[7] Having an effective, efficient, and precise method of measuring free T would help to determine how much T is readily available for use by the body in a specific patient. In one study, *Mellstrom et al* discovered that free T levels, not serum T levels, are a positive, independent predictor for osteoporosis related fractures in elderly men.[8] One personal hypothesis is that the levels of free T could also help identify any issues with the transport proteins associated with T delivery. If a patient was classified with normal levels of T by the serum testosterone test, but expressed low levels of free T, it may be concluded that the transport proteins are binding T but not releasing it properly. These types of issues could very well be detected using a sensor designed to only detect free T in an efficient and precise manner. The research presented below focuses on one such sensor, using silver colloid nanoparticles and well-known host-guest chemistry. An example of the process that would occur with a generic version of this sensor is displayed in figure 2.

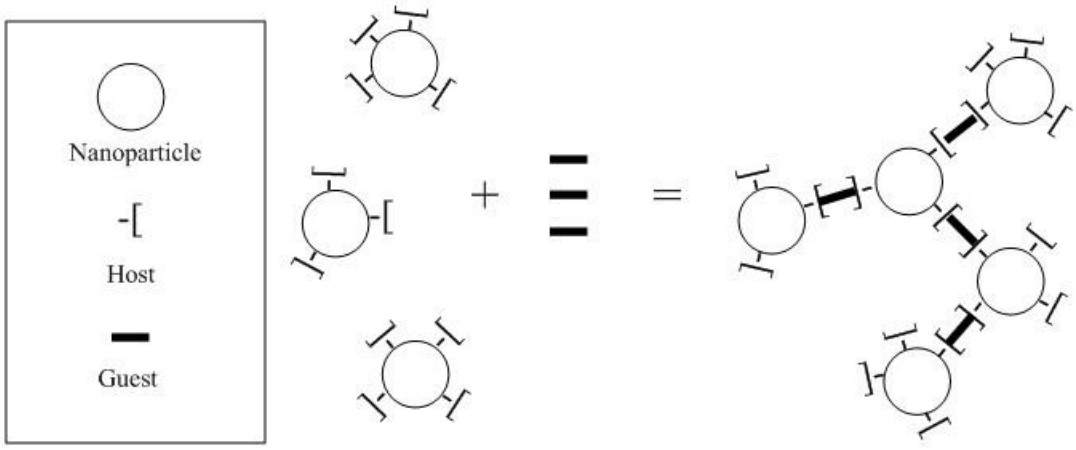

Figure 2: Depiction of the aggregation system presented in this research. The host molecule acts as both the capping agent and host, where the guest molecule acts as a link between nanoparticles. The silver particles provide the optical characteristics necessary to measure changes in the system.

Silver Colloid Nanoparticle Characteristics

Metallic nanoparticles have been widely discussed due to their versatile chemical properties. They have already been discovered to have antimicrobial activity as well as applications for nanotechnology and catalysis.[9,10] Aside from these applications, researchers have examined gold and silver nanomaterials due to their special optical characteristics. Most importantly, silver nanoparticles scatter light within the visible spectrum, allowing scientists to measure their optical characteristics using standard UV-Visible light spectroscopy. They do not absorb light, but rather scatter it because of their metallic surfaces. This scattering of light is more commonly known as Localized Surface Plasmon Resonance or LSPR. A simple graphical representation of LSPR and light scattering is located in figure 3.

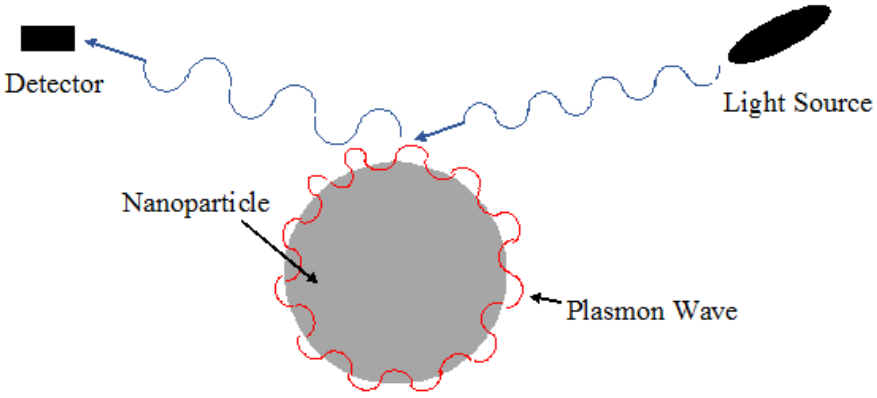

Figure 3: Visual representation of LSPR scattering of an incident photon of light

LSPR occurs when the incident photon of light entering a colloid nanoparticle solution is scattered by the metallic surface of the particles at a wavelength maximum. This maximum occurs when the photon of light and the surface plasmon of the particles are in resonance. In general, the surface plasmon is the oscillation of electrons along the surface of the metal. The LSPR can be measured as the wavelength of maximum scattering by standard UV-Vis spectroscopy. LSPR is an important method for measuring changes in nanoparticle composition because it is heavily dependent on the size and shape of the particles. As the particles change, the surface plasmons change, resulting in different maximum wavelengths.

There are several examples in which both size and shape affect the LSPR band of silver colloid nanoparticles. In an experiment performed by *Frank et al*, the size of silver colloid nanoprisms was adjusted independently of shape by varying the molar ratio between the silver nitrate added and the potassium bromide added. The sodium citrate (capping agent) concentration was kept constant. In general, a capping agent acts to terminate the nano metallic

growth of the particles. By varying the concentration of the potassium bromide, Frank controlled the size of the particles. The bromide ions inhibited growth of the particles in one direction, leading to the formation of variously sized silver nanoprisms rather than spheres. The results showed that by decreasing the amount of potassium bromide, the particles became larger resulting in the spectrum becoming red-shifted.[11] As the size of the particle increased the surface plasmon wave length increased, resulting in a longer/higher scattered wavelength detected by the spectrometer. Inversely, higher concentrations of potassium bromide reduced the size of the particles, resulting in a blue-shift or decrease in maximum wavelength.

The way in which the shape of the particle affects LSPR is somewhat more complicated than size changes. Particles synthesized by using various different techniques can have differences in shape and optical characteristics.[12] Nanospheres have been determined to be fairly simple to experiment with and a theory called the Generalized Lorenz-Mie theory (GLMT) has been developed to predict their scattering spectra.[13] They are known to give only one peak in UV-Vis spectroscopy because of their symmetric shape. Other shapes with more complicated geometry have been found to scatter light in more unique ways. For example, the amount of geometrical faces that exist on a particular particle structure will affect how many peaks appear on the spectrum due to the incident light scattering off multiple different faces of the particles. A sphere has one face and a rod has two geometric faces, therefore, nanorods display two peaks in the visible light spectrum.

In the same study mentioned above, Colby discusses how the dielectric constant of the surrounding environment may also affect the LSPR band of silver nanoparticles. The dielectric constant or charge of the surrounding medium affects the surface plasmon thus affecting the LSPR band. To avoid complications associated with using multiple-faced nanoparticles as well

as the dielectric constant of the solvent system, I focused my research on changes of simple nanospheres via particle aggregation in Millipore, or pure, water.

Nanoparticle Aggregation and Disaggregation

Both the aggregation and disaggregation of nanoparticles have been experimented with to determine their viability to act as bio or chemo sensors. As stated by *Wang et* al, gold nanorods can be used as a method for detecting analyte concentration.[14] This experiment involved aggregating gold nanorods in side-to-side and end-to-end conformations using antibody/antigen interactions. The antibody was bound to the nanorods and once its specific antigen was added to the solution, the rods began to disaggregate due to chemical competition. This resulted in a blue-shift in the LSPR band of the solution. On the other hand, in an experiment performed by *Liu et al*, gold nanospheres were aggregated by capping β-cyclodextrin (BCD) to the particles and introducing a ferrocene derivative to the system.[15] Ferrocene acted as a linker between particles due to its ability to form 1:2 complexes with BCD. The results from this experiment displayed a red-shift in the LSPR band of the particles and eventually a red solid precipitated out of solution verifying a large amount of particle aggregation. Using this experiment as a model system, I was able to incorporate host-guest chemistry into my potential biosensor system.

Host-guest Chemistry

The most common molecules used in host-guest chemistry are known as cyclodextrins. As mentioned before, β-cyclodextrin (BCD) is one such molecule. The chemical structure of BCD can be found in chart 1. BCD and other cyclodextrins act as the host molecules in the host-guest complex. These molecules rely on their chemical structure to form interactions between guest molecules. BCD has a 7 ring structure with several hydroxyl groups (primary and secondary). Its chemical structure and chirality result in a lipophilic inner cavity and hydrophilic

outer surface. This unique structure allows BCD to form noncovalent inclusion complexes with hydrophobic compounds that geometrically fit inside the lipophilic cavity.[16] Another important factor of BCD is its rigidity. The rigid structure of BCD due to its cyclohexane rings limits the mobility of the molecule once attached to silver nanoparticles. Structurally, testosterone can only be included into BCD molecules located on different nanoparticles. This eliminates any issues with the inclusion of T by two BCD molecules located on the same particle. To recap, silver nanoparticles capped with BCD may aggregate after introducing the steroid molecule testosterone, which would effectively act as a guest molecule and link between particles.

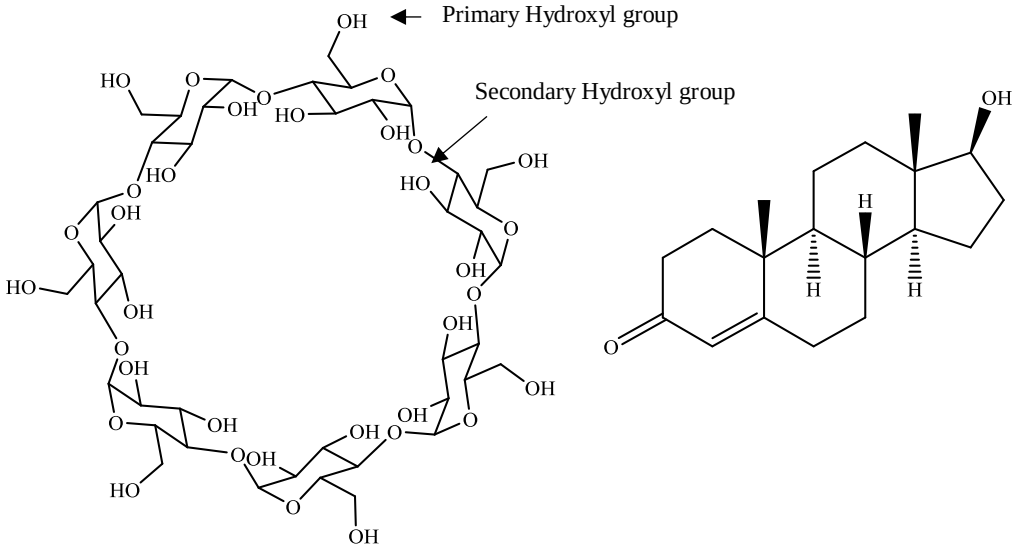

Chart 1: BCD (left) and Testosterone (right) structures

Prior research has already revealed successful complexation between steroids and BCD. Using phase-solubility and spectroscopic techniques, researchers have discovered that four specific steroids complex with BCD in a 1:2 steroid:BCD ratio suggesting that BCD capped nanoparticles should aggregate after the addition of a steroid molecule.[17] It was determined that the five-member ring of testosterone interacts with the lipophilic pocket of one BCD molecule first, then the 1:1 complex subsequently interacts with another BCD molecule. In other words, the reaction between the three molecules is stepwise. More specifically, the interaction between

the five membered ring of the steroid molecule and the first BCD molecule is thermodynamically favored over the 1:1 complex interaction with the second BCD molecule. Proper time is required to see the formation of the 1:2 complex. This research has also revealed that progesterone has the highest association constant with the lowest aqueous solubility. The order of the chemical characteristics between the four steroids tested is as follows; highest to lowest association constants: progesterone > cortisone > testosterone > hydrocortisone and highest to lowest aqueous solubility: hydrocortisone > cortisone > testosterone > progesterone.[17] Since my research has primarily been done in an aqueous environment, I decided to focus on testosterone due to its biochemical significance and higher aqueous solubility than progesterone. The aqueous solubility of testosterone is very low at less than 1 mL/L v/v as displayed by sigma Aldrich. Refer to chart 1 for the molecular structure of testosterone.

Synthesis of BCD capped Nanoparticles

As stated before, I synthesized silver nanoparticles capped with BCD in order to effectively use host-guest interactions to aggregate the particles. Silver colloid nanoparticles are very easily formed using methods that most commonly include silver nitrate, a capping agent, and a reducing agent. The reducing agent's function is to reduce silver nitrate to neutral silver forming nucleation sites in the solution. The balanced reduction reaction of silver nitrate is displayed in scheme 1. This reduction reaction includes one of the most common reducing agents, sodium borohydride ($NaBH_4$), however, there are several other reducing agents including sodium citrate and even plant extract antioxidants.[18,19]

Scheme 1:

$$NaBH_{4\,(aq)} + 8\ AgNO_{3\,(aq)} + 4\ H_20_{\,(l)} \longrightarrow Na[B(OH)_4]_{\,(aq)} + 8\ Ag_{\,(s)} + 8\ HNO_{3\,(aq)}$$

The neutral silver atoms are drawn to each nucleation site, forming larger particles. Depending on the concentration and strength of the reducing agent, the amount of nucleation sites can be larger or smaller. This affects both the number of particles and the size of the particles. A higher number of nucleation sites will lead to a higher number of small particles due to increased competition between the free silver in the solution and the nucleation sites they are attracted to. The capping agent of the reaction binds to the growing particles, effectively stopping growth as well as stabilizing the particles. Depending on the capping agent as well as the concentration of the capping agent, the shape of the particles can be controlled. This has become one focus of my research; to further understand the ability of host molecules such as cyclodextrins to effectively cap and stabilize silver nanoparticles.[20]

As mentioned above, synthesis of silver nanoparticles requires a capping agent in the reaction in order to stabilize. BCD can be directly attached to silver nanoparticles as the capping agent in the reaction.[20] As the free silver in solution is aggregating around the nucleation sites created from the reduction reaction, the primary hydroxyl groups of BCD molecules interact with the metal and form covalent bonds to effectively stop the growth of the metal. The research done by *Andrade et al* included the use FTIR analysis, revealing C-O stretching of the primary hydroxyl groups of BCD. This finding allowed them to conclude that these hydroxyl groups are reactive with the silver nanoparticles.[21]

Centrifugation of Silver Nanoparticles

The centrifugation and cleaning of nanoparticles is a crucial aspect of researching with metallic particles. The synthesis method used to form such particles may leave excess reactants which can interfere with the chemical properties of the system. In the case of studying the bio or chemo sensing characteristics of nanoparticles, it is especially important to rid the test sample of

excess reactants to ensure the accuracy of the sensor. BCD acts as the host molecule for the proposed sensor above and in the reaction, excess is used to ensure proper capping of the nanoparticles. Free BCD in the solution may interact with testosterone as well as the bound BCD, causing inaccurate measurements of the concentration of testosterone.

There are several methods of cleaning silver nanoparticles that are used, most of which include the centrifugation and resuspension of nanoparticle pellets.[20,22] In the study by *Amiri et al* states, they discovered that cyclodextrin-capped nanoparticles are more difficult to centrifuge than particles capped with smaller molecules. Thus, these particles require additional centrifugation at high relative centrifugal force (RCF). Other studies use methods including the addition of acetone to reduce centrifugation time and speed required.[22, 23] This literature revealed that the capped-particles were less soluble in acetone if the capping agent itself was less soluble in acetone, resulting in the separation of the particles from the supernatant. Since the solubility of BCD decreases with an increase in the mole fraction of acetone in the solution, this technique was used to separate the nanoparticles from the solution containing free BCD.[24] BCD was soluble in the acetone/water ratios used, so free BCD would not precipitate out with the nanoparticles. This technique is primarily used if the size of the nanoparticle is small. Larger nanoparticles are more easily separated due to their size and weight.

Ultimately, BCD-capped nanoparticles show the potential to effectively detect the concentration of free testosterone in vitro by examining red-shifts in the LSPR band of the colloidal suspension. BCD has already been found to both effectively cap nanoparticles as well as complex with testosterone. Some limitations of this work may include difficulties with the solubility of testosterone as well as selectivity. Since it is known that BCD also forms complexes with other steroid derivatives, this research falls more closely under the scope of a

proof-of-concept experiment and will ideally lead to further research. This biosensor system could potentially be used to detect low levels of free T effectively determining whether a patient's free testosterone levels are at a healthy level and that the transport proteins associated with this hormone are functioning properly.

Experimental Methods:

Materials

For the procedures listed below, the following chemicals were used. Silver nitrate from Acros Organics with a purity of 99+%, sodium borohydride from Acros Organics with a purity of 98+%, and pure β-Cyclodextrin from Alfa Aesar Chemicals were used in the synthesis of silver nanoparticles. Testosterone EIA standards (50 ng/mL in ethanol) from the Cayman Chemical Company were used for the testosterone analysis samples. Reichstein's Substance s from Sigma Aldrich with a purity of 98+% was used as a testosterone derivative.

Hazards

Testosterone EIA Standard – Highly flammable (category 2), can cause skin and eye irritation (category 2), potential damage to fertility (category 2 reproductive toxicity), may cause respiratory irritation or drowsiness and dizziness from single exposure (category 3 Target Organ Systemic Toxicity), and may cause damage to target organs through repeated exposure (Category 1 Target Organ Systemic Toxicity). Keep away from flames and wear protective gloves/clothing and eye/face protection. All safety information has been reported from the safety data sheet as provided by the Cayman Chemical Company.

Silver Colloid Nanoparticle Preparations

An array of silver nanoparticle colloid solutions was prepared using sodium borohydride as the reducing agent and β-cyclodextrin as the capping agent.[20] A tabular representation of the

solutions prepared is located in table 1. At first, a solution of sodium borohydride was prepared in Millipore water and stored at 4˚C for 30 minutes. During this time, a solution of silver nitrate and β-cyclodextrin was prepared in Millipore water and stirred until the reagents were completely dissolved. While the solution was stirring, the chilled sodium borohydride was added and the solution turned to a clear yellow color. The solution was allowed to stir overnight to ensure the reaction reached completion. The colloidal suspensions were stored in plastic bottles and were stable for up to a year. The spectrum of each sample was taken using a PerkinElmer Lambda 650 spectrometer to measure potential shifts in the maximum wavelength.

Table 1: Final concentrations of silver nitrate, β-cyclodextrin, and sodium borohydride in each sample of silver colloids prepared.

Solution Number	[$AgNO_3$] (mM)	[BCD] (mM)	[$NaBH_4$] (mM)	λ_{max} (nm)
1	0.1	6.0	5	401.36
2	0.1	4.0	5	399.87
3	0.1	2.0	5	399.20
4	0.2	2.0	5	397.12
5	0.4	2.0	5	Saturated
6	0.2	2.0	2.5	396.94
7	0.2	2.0	1.0	393.51
8	0.2	2.0	0.5	389.59

Centrifugation of Nanoparticles

For the remainder of the experiment, the 0.2 mM $AgNO_3$, 2.0 mM BCD, and 2.5 mM $NaBH_4$ colloid solution was used. Several centrifugation techniques were used to pellet and clean the nanoparticles.[20, 22, 23] One specific centrifugation technique was attempted by using acetone to stimulate pelleting.[23] A mixture of 50/50 acetone:colloid was created and centrifuged at 38,724 RCF or relative centrifugal force for 15 minutes using a Du Pont Instruments Sorvall RC-5B Refrigerated Superspeed Centrifuge and Sorvall SS-34 rotor. The amount of colloids used per centrifugation never exceeded 5 ± 0.02 mL for a total of 10 mL in solution. A balance tube was created by ensuring the weights of each tube were the same. A colloidal film formed

on the tube and was re-suspended in Millipore water (3 ± 0.02 mL) following the decantation of the supernatant.

Testosterone Assays

Several assays of testosterone samples were created by mixing varying amounts of testosterone with colloidal suspensions. Testosterone standards (50 ng/mL) in ethanol were used to create these samples. The T standards were stored at 4˚C when not in use. Varying volumes of the testosterone standard were added to a constant volume of the colloidal solutions (400 µL) to imitate a range of physiologically relevant testosterone concentrations. The testosterone concentrations ranged from 1 ng/mL to 10 ng/mL. The samples were diluted to a final volume of 500 µL with Millipore water. In addition, ethanol standards were prepared using the same procedure as mentioned above to ensure the trends observed were not a result of the solvent. The volume of ethanol added to each sample corresponded with each testosterone sample mentioned above. To test both reproducibility and selectivity, a testosterone derivative was also tested using the aforementioned procedure. The UV-Visible light spectra for each sample were collected after the samples equilibrated for 48 hours.

Results:

The spectra presented below have two peaks, each with their own potential changes as a function of testosterone. To begin, Figure 4 below displays an overlay of the UV-Visible spectra for the testosterone samples baselined to the lowest tail-end value of the samples. There is an overall increasing trend of the extinction at the main peak in the 400 nm range between 0 ng/mL to 4 ng/mL. At 5 and 10 ng/mL, however, there was a decrease in the extinction compared to the previous samples.

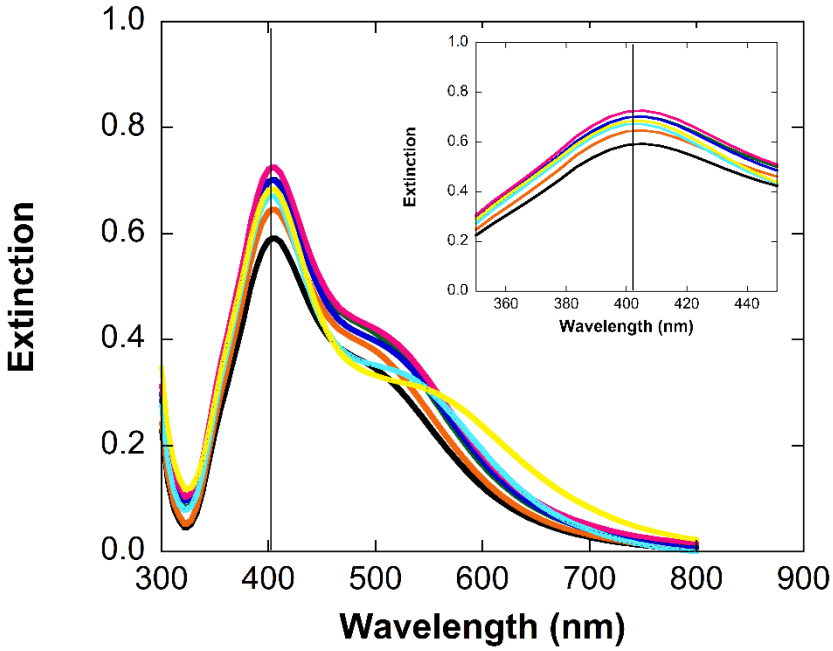

Figure 4: Spectrum overlay of testosterone samples. The black, orange, green, blue, pink, light blue, and yellow lines represent samples 1 (0 ng/mL T), 2 (1 ng/mL T), 3 (2 ng/mL T), 4 (3 ng/mL T), 5 (4 ng/mL T), 6 (5 ng/mL T), and 7 (10 ng/mL T) respectively.

To further examine any changes happening in the system, specifically in the area around 488 nm, all of the graphical data were normalized at the main peak to determine any changes in the second peak region that may result in a linear trend. These data are represented graphically in figure 5 below.

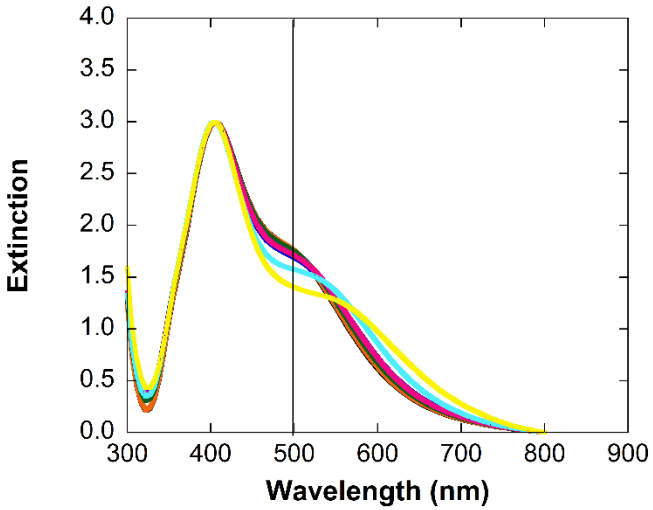

Figure 5: Normalized spectrum overlay of testosterone samples. The black, orange, green, blue, pink, light blue, and yellow lines represent samples 1 (0 ng/mL T), 2 (1 ng/mL T), 3 (2 ng/mL T), 4 (3 ng/mL T), 5 (4 ng/mL T), 6 (5 ng/mL T), and 7 (10 ng/mL T) respectively.

In both figures 4 and 5, the main peak in the 400 nm range represents the majority of colloidal silver and the secondary peak indicates irreversibly aggregated particles caused by centrifugation and interaction with BCD. To examine the effects T has on the system in a quantifiable way, changes in the normalized extinction of the shoulder peak of the spectrum at 488 nm as well as the shape of the two Gaussian peaks that make up each spectrum were examined. Indicated by the graphs above, there appeared to be a clear "stretching" of the shoulder peak. This fact can be coupled with the decrease in the normalized extinction of this peak for each addition of testosterone. Figure 6 displays the change in the extinction as a function of the concentration of testosterone in each sample.

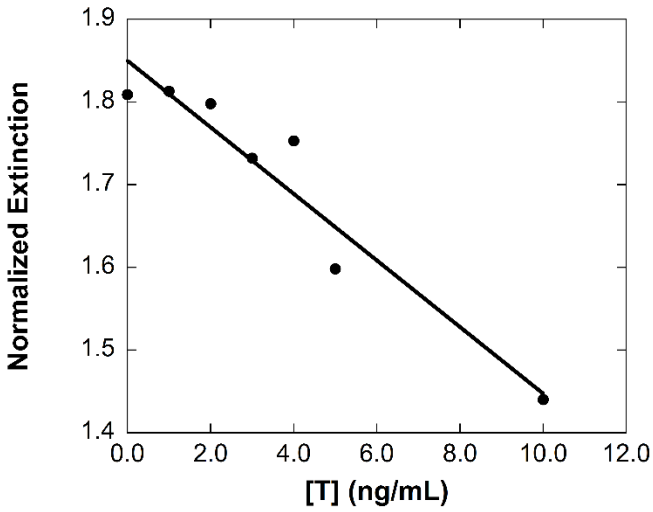

Figure 6: Graphical representation of the normalized extinction value of the secondary colloidal peak at 488 nm as a function of the concentration of testosterone. Solid circles represent the apparent second peak extinction as a function of testosterone concentration. The solid line represents a line of best fit with a slope of -0.04027/(ng/mL) and a y-intercept of 1.85.

Figure 6 displays the extinction values of the secondary colloidal peak at 488 nm normalized by the extinction of the main colloidal peak (399 nm) as a function of the testosterone concentrations. The fit-line has an R^2 value of 0.9593, indicating a linear relationship between the decrease in the normalized extinction of the secondary peak and the

concentration of testosterone. The lower point values between 0 and 2 ng/mL display little to no change in the extinction of this peak, meaning the detection limit of the sensor may be higher than 2 ng/mL. The detection limit of the traditional serum testosterone test is 0.36 ng/dL or 0.0036 ng/mL as reported in a laboratory procedure manual by the CDC, which is much lower than 1 ng/mL.[25]

To truly examine changes that were occurring to the shoulder peak, each spectrum was simulated as the sum of two overlapping Gaussian peaks. The general equation for a Gaussian curve is shown in equation 1.

$$Gaussian\ Peak = ae^{\frac{-(x-<x>)^2}{2\sigma^2}} \quad (1)$$

The "a" coefficient represents the peak height, the <x> variable represents the peak center and the sigma (σ) represents the full width of the peak at half the maximum height (FWHM). By adjusting these variables for two peaks, the spectrum for each sample could be mathematically simulated.

From these calculations, there was no apparent shift of the true maximum wavelength of the shoulder peak, however, there was a consistent increase in the width of the second Gaussian peak. The parameters that fit each of the spectra in figure 4 are located in table 2.

Table 2: Data gathered from Gaussian peak simulations

Sample	[T] (ng/mL)	Center of First Peak (nm)	Width of First Peak (nm)	Center of Second Peak (nm)	Width of Second Peak (nm)
1	0	399	32	488	75
2	1	399	32	488	75
3	2	399	32	488	80
4	3	399	32	488	85
5	4	399	32	488	88
6	5	398	32	490	106
7	10	400	32	495	130

There is a fairly consistent increase in the peak width of the second Gaussian peak until the 5 ng/mL sample, where the increase becomes more drastic. There are slight fluctuations in the location of the peak center for the first peak as well as a clear increase in wavelength of the second peak center at the 5 and 10 ng/mL mark. This may be an indication that this system may be better at detecting higher levels of testosterone rather than small values. To further examine the trend between the second Gaussian peak width and the concentration of testosterone, a graph was created and displayed in figure 7.

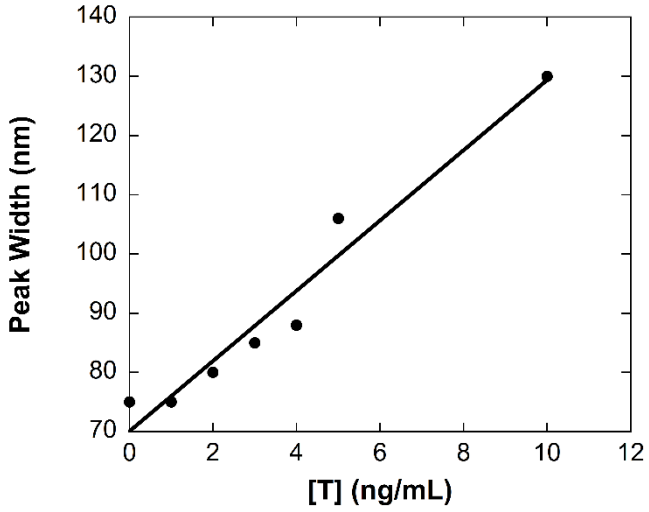

Figure 7: Graphical representation of the peak width (nm) of the second simulated Gaussian peak as a function of the concentration of testosterone. Solid circles represent the apparent second peak's peak width as a function of testosterone concentration. The solid line represents a line of best fit with a slope of 5.9326 nm/(ng/mL) and a y-intercept of 70.098 nm.

The fit-line of this equation is linear and has an R^2 value of 0.97692. No statistical analysis could be carried out on this distribution due to the lack of additional trial data.

To ensure these trends were not due to the addition of ethanol to the system, a set of ethanol only samples was created and displayed as a spectra overlay in figure 8. There was no clearly substantial shift in the normalized extinction of the secondary peak as a function of the concentration of ethanol.

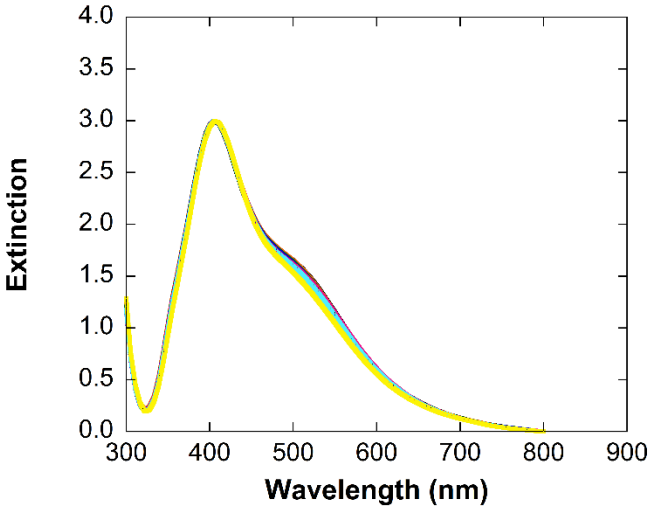

Figure 8: Spectrum overlay of ethanol samples. The black, orange, green, blue, pink, light blue, and yellow lines represent samples 1 (0% EtOH), 2 (2% EtOH), 3 (4% EtOH), 4 (6% EtOH), 5 (8% EtOH), 6 (10% EtOH), and 7 (20% EtOH) respectively. These ethanol percentage directly correspond with the amounts of ethanol in each of the testosterone test samples.

One additional test assay was run using Reichstein's substance S (RS-s), a slightly more polar derivative of testosterone to examine the selectivity of the sensor. A spectra overlay of these samples is represented graphically in figure 9.

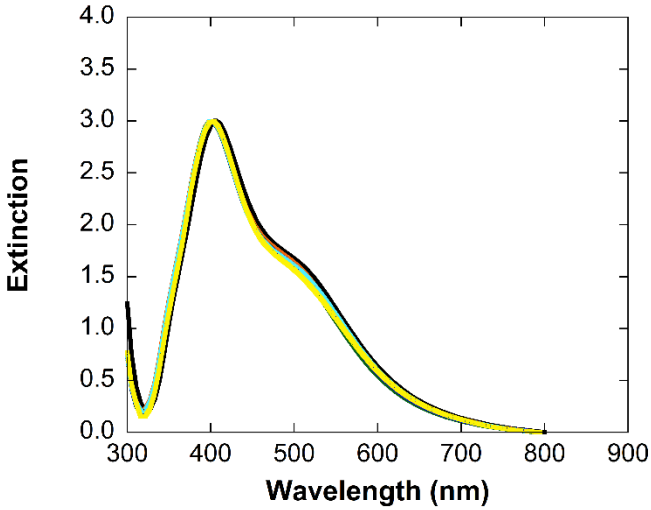

Figure 8: Spectrum overlay of Reichstein's substance S samples. The black, orange, green, blue, pink, light blue, and yellow lines represent samples 1 (0 ng/mL RS-s), 2 (1 ng/mL RS-s), 3 (2 ng/mL RS-s), 4 (3 ng/mL RS-s), 5 (4 ng/mL RS-s), 6 (5 ng/mL RS-s), and 7 (10 ng/mL RS-s) respectively.

As Compared to the testosterone samples, Reichstein's substance S did not seem to complex with the BCD-capped particles nearly as well. There are very slight shifts if any at all with no conclusive trend. Any minor shifts that occurred can be attributed to the slight effects ethanol has on the system.

Discussion:

The results presented above display trends that show a correlation between the concentrations of testosterone for each sample as a function of the changes in the optical characteristics of the silver nanoparticles. The spectral overlays display these changes graphically and indicate that there were changes in the baselined extinction of the 399 nm peak as well as the normalized extinction of the secondary peak with varying concentrations of testosterone. Although there was not a linear trend associated with the increase in extinction of

the main peak, these results offer an interesting look at how this system changes in relation to testosterone concentration.

The trend associated with the decrease in the normalized extinction of the shoulder peak can be further examined due to fact that the peak width of the second simulated Gaussian peak also increased with the addition of higher concentrations of T. Mathematically, these trends pair nicely together if we assume that the number of particles represented by the area under the aggregate peak (488 nm) remains constant. With this in mind, as the distribution of the peak becomes wider, the peak value or extinction value must decrease to maintain the same total area under the peak. These trends suggest that the interaction between BCD and testosterone is further aggregating or disaggregating the particles that were already aggregated through centrifugation and not interacting strongly with the un-aggregated particles at 399 nm.

A chemically relevant explanation for these phenomena is that the irreversibly aggregated particles caused by the centrifugation of the colloids interacted with testosterone and created nanoparticle aggregates with a large distribution of sizes. The aggregates caused by centrifugation were most likely interacting between the secondary hydroxyl groups of the β-Cyclodextrin molecules attached to the particles. Following the introduction of testosterone to the system, these aggregates may break apart or grow in size due to the fact the testosterone will interact with BCD along with BCD interacting with other BCD molecules. The end result of this was the formation of larger as well as smaller aggregates as seen by the stretching of the shoulder peak. This is caused by the linkage of particles through the complexation of T and BCD. The interpretation associated with the disaggregation and re-aggregation of the shoulder peak nanoparticles is consistent with the increase in peak width in conjunction with the decrease

in the normalized extinction at 488 nm. This interpretation also pairs well with the step-wise guest-host binding mechanism identified by *Liu et al*.[17]

The increase in peak width may also play a part in the optical changes observed at the 399 nm peak. As the aggregated particle distribution becomes wider, there will be a corresponding increase in the extinction of the 399 nm peak because the secondary peak has more of an effect on the overall shape of the resulting spectra. This helps explain why there was an increase in extinction between the 0 ng/mL sample and the 4 ng/mL sample. In terms of the higher testosterone concentration samples, there appeared to be a decrease in extinction in comparison to the lower testosterone concentration samples. One potential interpretation of this occurrence may be that the aggregated particle distribution began to favor the higher end of the spectrum or larger aggregates at these testosterone levels. In other words, with the addition of more testosterone, larger particle aggregates were more prominent than smaller particle aggregates. These results do not form a measurable trend, however, they do offer additional proof of the effects testosterone had on the colloidal silver.

The test assay involving Reichstein's substance S displayed no such trends. This molecule has a different substituent on the five carbon ring of the compound that has several polar oxygen groups. The polarity of this substituent may interfere with its complexation with BCD, preventing aggregation due to the failed formation of a 1:2 complex between RS-s and BCD. This fact also relates to the step-wise binding method mentioned previously.[17] The molecular structure of RS-s can be found in chart 2.

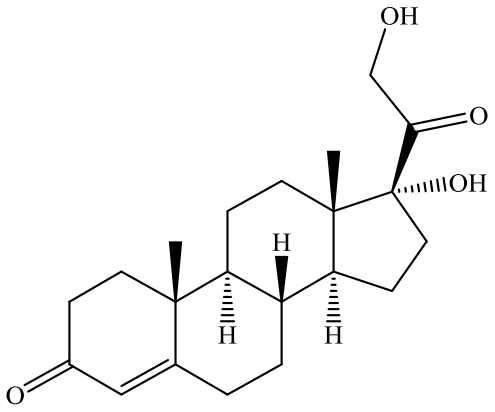

Chart 2: Structure of Reichstein's Substance s

Overall, when T is introduced, there is a fairly clear broadening and a red-shift of the maximum wavelength of the secondary peak indicating the formation of larger aggregates than that of the centrifuged aggregates. More specifically, the peak appears to stretch down the spectrum which shows the formation of aggregates of a non-universal size. The trend-line shows that the relationship between this increase in peak width size and the concentration of testosterone is linear. This experiment and the linearity of the trend-line may lead to the formation of a very simple calibration curve, which can be used to determine the testosterone concentration using either the normalized absorbance at 488 nm or the peak width of the second simulated Gaussian peak. It is an intriguing finding that further shows the potential capabilities of silver nanoparticles to act as a biosensor for testosterone.

Examining the raw data of the experiment shows that the detection limit of the sensor may fall somewhere between 1 and 4 ng/mL of testosterone. There were fairly inconsistent shifts of the LSPR of the secondary peak between these points. Based on 1 trial, there was no shift between no testosterone and 1 ng/mL T, yet there was a shift between 1 and 2 ng/mL T followed by a minimal shift between 3 and 4 ng/mL T. The sensitivity of this sensor is still a

fairly large concern due to the accuracy of the serum testosterone test as presented above. The average concentration of serum testosterone in healthy men is approximately 500 ng/dL or 5 ng/mL, where the concentration of free T is much lower at under 1 ng/mL, a value under the apparent detection limit of this sensor.[26] With multiple trials, more accurate numbers can be developed using averages as well as error bars; however, the discrepancies presented with 1 trial make it very difficult to determine the true detection limit of the sensor.

Some of the limitations of this work include reproducibility and sensitivity due to issues with the vast number of variables that may affect the overall outcome of the experiment. Silver colloid nanoparticles have simple synthesis methods, however, the concentrations of each reagent drastically affect the size and shape of the particles. This may lead to difficulties in reproducing particles of the same size and shape as a previous test sample. Also, the centrifugation techniques used resulted in fairly inconsistent pelleting of the particles depending on the particle variables as mentioned before. This may lead to uneven particle distribution due to the pelleting of large particles while smaller particles remain in the supernatant. All of these factors may affect the results of the testosterone assays and adjust the make-up of the calibration curve. It is shown that nanoparticles attached with BCD begin to aggregate on their own over a fairly long span of time, however, completing experiments quickly may offer a solution to issues with inconsistent particle size.[20] As for issues with shape, there are more synthesis methods that may result in more consistent shape distributions, however, the addition of BCD would have to occur either after the silver nanoparticles have been synthesized or be a replacement reagent for the capping agent.[11] In terms of sensitivity, synthesizing particles of a larger size may remedy this issue by increasing the ease of aggregation.

One other limitation is primarily caused by the fact that the solubility of testosterone in water is very low. The testosterone standards were prepared in ethanol, a known etching agent of silver nanoparticles. Etching agents are capable of adjusting the shape of nanoparticles, thus changing the optical characteristics.[27] There were fairly minimal shifts in the LSPR as a result of ethanol and high concentrations of ethanol would not be located in actual biological samples, thus this issue may not pose a problem in the future.

Further research is required to examine the reproducibility and accuracy of the experiment. Due to the many factors involved in changing the optical characteristics of silver nanoparticles, more trials should be done to determine the optimal size and shape for use as this type of biosensor. Larger sized particles may result in a more sensitive system due to an increased ease in aggregation. The specificity of the biosensor must also be assessed. BCD is known to complex with several hormone and steroid derivatives, thus making it a fairly indiscriminant biosensor. That being said, BCD interacts with steroid and hormone molecules in a very specific stepwise mechanism. The results presented by the RS-s trial show that the polarity of the substituent on the five-membered ring of the molecule is very important for successful complexation of BCD with the guest molecule. Steroids such as progesterone and cortisone have fairly nonpolar substituents, making them the most likely to interfere with testosterone testing.

Conclusions:

The results presented in this report demonstrate the ability of colloidal silver to act as a biosensor for the steroid testosterone. There was a clear, experimentally determined trend between two aspects of the optical characteristics of the particles as a function of the concentration of testosterone. These trends were mathematically analyzed and followed normal mathematical trends. Not only are these shifts associated with the aggregation of silver nanoparticles due to host-guest chemistry, but they are also supported by the literature presented in the report. Although the results were based off of one trial, further research into this concept may reveal additional proof of the potential silver colloids have in acting as a biosensor for testosterone.

Bibliography

1. Durant, Robert, Vaughn Rickert, Carolyn Ashworth, Cheryl Newman, and Gregory Slavens. 1993. "Use of Multiple Drugs among Adolescents Who use Anabolic Steroids." *The New England Journal of Medicine*.

2. Assmann, Gerd and Antonio M. Gotto Jr. 2004. "HDL Cholesterol and Protective Factors in Atherosclerosis." *Circulation* 109: 14.

3. Nguyen, Ray. "The Science Behind Testosterone Biomarkers." InsideTracker., last modified Feb 26, accessed Nov 13, 2016.

4. Fennell, Michael and Colin Scanes. 1991. "Effects of Androgen (Testosterone, 5 - Dihydrotestosterone, 19-." *Physiology and Reproduction*.

5. Gottlieb, Bruce, Rose Lombroso, Lenore K. Beitel, and Mark A. Trifiro. 2005. "Molecular Pathology of the Androgen Receptor in Male (in)Fertility." *Reproductive BioMedicine Online* 10 (1): 42-48.

6. Lynne V. Nazareth and Nancy L. Weigel. 1996. "Activation of the Human Androgen Receptor through a Protein Kinase A Signaling Pathway." *Journal of Biological Chemistry* 271 (33): 19900-19907.

7. Vermeulen, A., L. Verdonck, and J. M. Kaufman. 1999. "A Critical Evaluation of Simple Methods for the Estimation of Free Testosterone in Serum." *The Journal of Clinical Endocrinology and Metabolism* 84 (10): 3666-3672.

8. Mellström, Dan, Olof Johnell, Östen Ljunggren, Anna-Lena Eriksson, Mattias Lorentzon, Hans Mallmin, Anna Holmberg, Inga Redlund-Johnell, Eric Orwoll, and Claes Ohlsson. 2006. "Free Testosterone is an Independent Predictor of BMD and Prevalent Fractures in Elderly Men: MrOS Sweden." *Journal of Bone and Mineral Research* 21 (4): 529-535.

9. Sondi, Ivan and Branka Salopek-Sondi. 2004. "Silver Nanoparticles as Antimicrobial Agent: A Case Study on E. Coli as A model for Gram-Negative Bacteria." *Journal of Colloid and Interface Science* 275 (1): 177-182.

10. Khouloud, Abou El-Nour, Eftaiha Ala'a, Al-Warthan Abdulrhman, and Ammar Reda. 2009. "Synthesis and Applications of Silver Nanoparticles." *Arabian Journal of Chemistry*.

11. Frank, Andrew J., Nicole Cathcart, Kenneth E. Maly, and Vladimir Kitaev. 2010. "Synthesis of Silver Nanoprisms with Variable Size and Investigation of their Optical Properties: A First-Year Undergraduate Experiment Exploring Plasmonic Nanoparticles." *Journal of Chemical Education* 87 (10): 1098.

12. Cobley, Claire, Sara Skrabalak, Dean Campbell, and Younan Xia. 2009. "Shape-Controlled Synthesis of Silver Nanoparticles for Plasmonic and Sensing Applications." *Plasmonics* 4 (2): 171-179.

13. Maheu, B., G. Gouesbet, and G. Grehan. 1988. "A Concise Presentation of the Generalized Lorenz-Mie Theory for Arbitrary Location of the Scatterer in an Arbitrary Incident Profile." *Journal of Optics* 19: 59.

14. Wang, Libing, Yingyue Zhu, Liguang Xu, Wei Chen, Hua Kuang, Liqiang Liu, Ashish Agarwal, Chuanlai Xu, and Nicholas A. Kotov. 2010. "Side-by-Side and End-to-End Gold Nanorod Assemblies for Environmental Toxin Sensing." *Angewandte Chemie (International Ed. in English)* 49 (32): 5472-5475.

15. Liu, Jian, Sandra Mendoza, Esteban Román, Matthew J. Lynn, Renliang Xu, and Angel E. Kaifer. 1999. "Cyclodextrin-Modified Gold Nanospheres. Host−Guest Interactions at Work to Control Colloidal Properties." *Journal of the American Chemical Society* 121 (17): 4304-4305.

16. Liu, Pei, Shan Sun, Xiaochen Guo, Xiaohai Yang, Jin Huang, Kemin Wang, Qing Wang, Jianbo Liu, and Leiliang He. 2015. "Competitive Host-Guest Interaction between B-Cyclodextrin Polymer and Pyrene-Labeled Probes for Fluorescence Analyses." *Analytical Chemistry* 87 (5): 2665.

17. F Y Liu, D O Kildsig, and A K Mitra. 1990. "Beta-Cyclodextrin/Steroid Complexation: Effect of Steroid Structure on Association Equilibria." *Pharmaceutical Research* 7 (8): 869-873.

18. Rashid, Mamun, Khairul Bhuiyan, and M. Quayum. "Synthesis of Silver Nano Particles (Ag-NPs) and their Uses for Quantitative Analysis of Vitamin C Tablets." .

19. Rodríguez-León, Ericka, Ramón Iñiguez-Palomares, Rosa Navarro, Ronaldo Herrera-Urbina, Judith Tánori, Claudia Iñiguez-Palomares, and Amir Maldonado. 2013. "Synthesis of Silver Nanoparticles using Reducing Agents obtained from Natural Sources (Rumex Hymenosepalus Extracts)." *Nanoscale Research Letters* 8 (1): 1-9.

20. Setareh Amiri, Laurent Duroux, and Kim Lambertsen Larsen. 2015. "Silver Nanoparticle Colloids with [Gamma]-Cyclodextrin: Enhanced Stability and Gibbs-Marangoni Flow." *Journal of Nanoparticle Research* 17 (1): 1.

21. Patricia Fernanda Andrade, Andreia Fonseca de Faria, Douglas Soares da Silva, Juliano Alves Bonacin, and Maria do Carmo Gonc¸alves. 2014. *Structural and Morphological Investigations of -Cyclodextrin-Coated Silver Nanoparticles*.

22. Mackey, Megan A., Farhat Saira, Mahmoud A. Mahmoud, and Mostafa A. El-Sayed. 2013. "Inducing Cancer Cell Death by Targeting its Nucleus: Solid Gold Nanospheres Versus Hollow Gold Nanocages." *Bioconjugate Chemistry* 24 (6): 897-906.

23. Chou, Kan-Sen and Chiang-Yuh Ren. 2000. "Synthesis of Nanosized Silver Particles by Chemical Reduction Method Q." *Materials Chemistry and Physics*.

24. Anthony W. Coleman, Marc Munoz, and Alexis K. Chatjigakis. 1993. "Classification of the Solubility Behaviour of B-Cyclodextrin in Aqueous-Co-Solvent Mixtures." *Journal of Physical Organic Chemistry* 6.

25. Vesper, Hubert. "CDC Laboratory Procedure Manual."

26. Harman, S. Mitchell, E. Jeffrey Metter, Jordan D. Tobin, Jay Pearson, and Marc R. Blackman. 2001. "Longitudinal Effects of Aging on Serum Total and Free Testosterone

Levels in Healthy Men." *The Journal of Clinical Endocrinology & Metabolism* 86 (2): 724-731.

27. Mulvihill, Martin J., Xing Yi Ling, Joel Henzie, and Peidong Yang. 2010. "Anisotropic Etching of Silver Nanoparticles for Plasmonic Structures Capable of Single-Particle SERS." *Journal of the American Chemical Society* 132 (1): 268